

(001) faceting and $\text{Bi}_2\text{Sr}_2\text{CuO}_{6+x}$ ($T_c = 7\text{--}22$ K) phase formation at the Ag/Bi-Sr-Ca-Cu-O interface in Ag-clad $\text{Bi}_2\text{Sr}_2\text{CaCu}_2\text{O}_{8+x}$ ($T_c = 75\text{--}95$ K) superconducting tapes

Y. Feng

Applied Superconductivity Center, University of Wisconsin, Madison, Wisconsin 53706

D. C. Larbalestier and S. E. Babcock

Applied Superconductivity Center and Department of Materials Science and Engineering, University of Wisconsin, Madison, Wisconsin 53706

J. B. Vander Sande

Department of Materials Science and Engineering, Massachusetts Institute of Technology, Cambridge, Massachusetts 02139

(Received 8 May 1992; accepted for publication 22 June 1992)

The Ag/Bi-Sr-Ca-Cu-O (BSCCO) interface in Ag-clad Bi-2212 tapes was investigated by high-resolution transmission electron microscopy. The interface was found to be well bonded and free of nonsuperconducting second phases. However, a one-half-unit-cell-thick layer of the Bi-2201 phase was observed between the Bi-2212 phase and the Ag-cladding. A very strong texturing of the (001) planes of the BSCCO parallel to the Ag was seen. When the interface was nearly parallel to the Bi-2212 (001) planes, it tended to facet onto (001), leaving steps of height equal to one-half the Bi-2201 lattice spacing. Thus, strong (001) texturing extends to the atomic scale.

Ag-clad tapes of Bi-cuprate superconductors made by the powder-in-tube process have shown great promise for applications as conductors in very high magnetic fields. Many laboratories¹⁻⁶ have obtained very high critical current densities in such tapes. However, it is still a challenge to reproduce these results in a consistent manner and in long lengths of tape.

The crystal structures of the Bi-Sr-Ca-Cu-O (BSCCO) system consist of perovskitelike units containing 1, 2, or 3 CuO_2 planes sandwiched between Bi-O bilayers.^{7,8} There are three superconducting phases in the BSCCO system: $\text{Bi}_2\text{Sr}_2\text{CuO}_{6+x}$ ($T_c = 7\text{--}22$ K), $\text{Bi}_2\text{Sr}_2\text{CaCu}_2\text{O}_{8+x}$ ($T_c = 75\text{--}95$ K), and $\text{Bi}_2\text{Sr}_2\text{Ca}_2\text{Cu}_3\text{O}_{10+x}$ ($T_c = 105\text{--}110$ K). For brevity, they are referred to as Bi-2201, Bi-2212, and Bi-2223, respectively. The lattice parameter along the c axis of these phases increases with increasing number of CuO_2 and Ca planes, i.e., $c = 2.4, 3.0,$ and 3.7 nm, respectively. Studies of the phase formation in the BSCCO system have been done by several groups.⁹⁻¹² However, details of the Bi-2212 and Bi-2223 phase formation are still obscure.

The influence of Ag in both $\text{YBa}_2\text{Cu}_3\text{O}_{7-y}$ (YBCO) and BSCCO tapes has been discussed by many groups.¹³⁻¹⁷ Kase *et al.*¹⁷ demonstrated that the melting point of the Bi-2212 phase was lowered and a highly textured microstructure was promoted when thick doctor-bladed films were partially melted in contact with Ag. This behavior was also observed in Ag-clad BSCCO tapes.^{1,3,13,14,18,19} However, the real role that Ag plays is not yet fully understood. One aspect that is still unclear is how and why Ag promotes grain alignment. To our knowledge, no detailed investigation of the microstructure of the Ag/BSCCO interface has been published. In this letter, we report on the nm-scale microstructure of the Ag/BSCCO interface in Ag-clad Bi-2212 tapes as revealed by high-

resolution transmission electron microscopy imaging (HRTEM).

BSCCO Ag-clad tapes with the stoichiometric 2:2:1:2 starting composition were prepared by a standard powder-in-tube method. The BSCCO powder¹⁹ was packed into a Ag tube (4.35 mm i.d., 6.35 mm o.d.) and then swaged to 3.28 mm o.d., drawn and rolled to rectangular tape 0.1 mm thick by 3 mm wide. The final BSCCO core thickness was 0.045 mm. The tapes were partially melted at 920 °C for 15 min, cooled at 240 °C/h from 920 to 840 °C, annealed at 840 °C for 70 h, removed from the furnace, and air cooled. All heat treatments were done in air.¹⁹ General details of the micro- and macrostructure and superconducting properties have been given previously.¹⁹

HRTEM samples showing the cross section containing the rolling direction (long axis of the tape) and the thin direction of the tape were made by gluing several tapes together along their broad faces. Slices were cut and ground to about 40 μm thick and were then mounted on gold grids.¹⁹ The samples were Ar-ion milled at 4.5 kV in a liquid nitrogen cooled stage and then examined in an Akashi 002B HRTEM.

Over 80% of the interface between the Ag and the BSCCO was found to be well bonded. The interface appears to be abrupt in the HRTEM images. Cracks were observed but it is uncertain whether or not these cracks were artifacts of sample preparation. The interface was always free of nonsuperconducting phases. A typical example is shown in Fig. 1. The Bi-O double layers, which appear as doubled dark bands in the high resolution images, abut the Ag at the interface. The interface is parallel to the (001) plane of BSCCO. It is also interesting to note that the separation between pairs of Bi-O double layers was found to only 1.2 nm immediately adjacent to the interface. This spacing equals one half of the c -axis length dimension

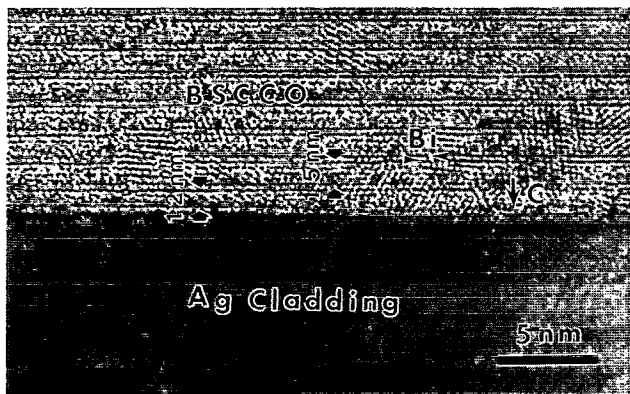


FIG. 1. A section of the Ag/BSCCO interface in the Bi-2212 Ag-clad tape processed by partial melting. A one-half unit cell thick layer of the Bi-2201 phase ($c/2=1.2$ nm) ending at the Bi-double layer is observed adjacent to the Ag cladding. The interface is parallel to the (001) plane of the BSCCO.

of the Bi-2201 phase. There is further evidence for this in Fig. 2, which shows the strong faceting that arises at interfaces that are slightly inclined to the (001) plane of the BSCCO. In order to maintain the (001) facets, a stepped microstructure develops, such that the step height equals one half of the Bi-2201 lattice spacing. The interface is well bonded on all facets.

Ag-BSCCO interfaces were also observed where Bi-2212 grains grew into the Ag cladding. Grains of this type, a few microns in length, were found. In such cases the major growth axis of the BSCCO grains is oblique to the Ag cladding. Figure 3 shows such a Ag/BSCCO interface formed by a large Bi-2212 grain ($\sim 1 \mu\text{m}$ wide by $\sim 15 \mu\text{m}$ long) which grew into the Ag cladding at an angle of $\sim 10^\circ$. Again it was observed that the interface lies parallel to (001) in the BSCCO and that a half unit cell thick Bi-2201 layer exists at the interface.

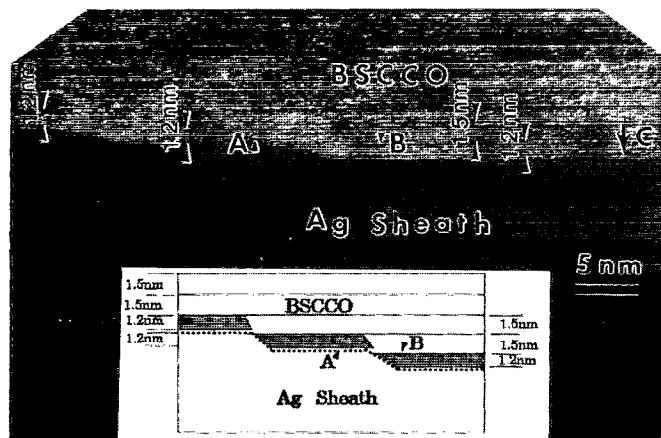


FIG. 2. A Ag/BSCCO interface in the Bi-2212 tape. This interface shows the strong faceting that arises at interfaces that are slightly inclined to the (001) plane of the BSCCO. A stepped microstructure develops, such that the step height equals one-half of the Bi-2201 lattice spacing. Note that the layer marked A B has the Bi-2201 spacing at A where it is immediately adjacent to the Ag but that this changes to the Bi-2212 spacing at B where it is no longer immediately adjacent to the Ag (see inserted schematic drawing).

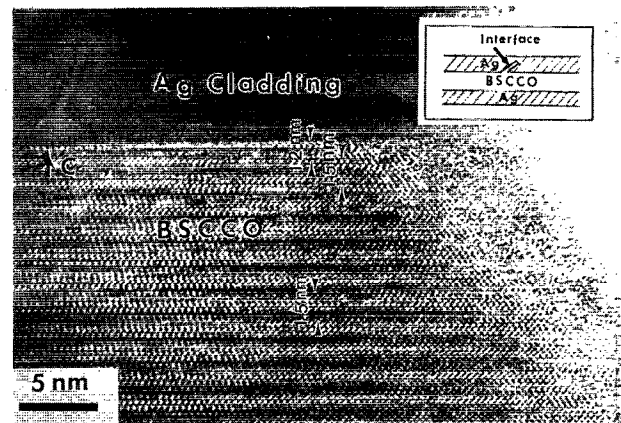


FIG. 3. A Ag/BSCCO interface formed by a large Bi-2212 grain ($\sim 1 \mu\text{m}$ wide by $\sim 15 \mu\text{m}$ long) penetrating the Ag cladding. The zone axis of the Bi-2212 grain is [110]. The one-half unit cell Bi-2201 layer is also observed at the interface.

The well-bonded interface between the Ag cladding and the BSCCO core, coupled with the fact that the interface always appears free of nonsuperconducting second phases, supports the general view that Ag is a desirable sheath material for producing BSCCO wires and tapes. The micrographs make it clear that there is a highly textured grain structure in which the a - b planes of the BSCCO phases are parallel to the Ag cladding. This is important because it is widely believed that the supercurrent is carried preferentially by the most highly aligned regions, among which are those layers which form next to the Ag. As seen from all three figures, a strong (001) faceting of BSCCO at the Ag interface occurs. Even for the obliquely aligned grains, the BSCCO still tends to maintain its (001) faceting accommodating small misalignments by leaving microsteps at the interface.

There are at least three questions posed by the present results. The first is the general question of why the (001) planes of the Bi-2212 phase tend to align macroscopically with the Ag. The rolling process tends to produce a powder that has its basal planes aligned along the plane of the tape. It is tempting to believe that this plays an important role in the final grain alignment, but Ray and Hellstrom²⁰ have recently shown that the 2212 phase is completely melted in tapes held at 920°C . Examination of tapes that have been rapidly quenched from just below the 2212 phase formation temperature shows a random nucleation of 2212 phase. With continued cooling, 2212 grains aligned parallel to the plane of the tape dominate the microstructure. Extended annealing at 840° increases this alignment. Evidently, the very much more rapid growth kinetics of the ab planes permits those grains with basal planes aligned close to the plane of the tape to consume some of the randomly aligned and shorter grains that first formed. Strong growth anisotropy is suggested by the deep penetration of the obliquely aligned grains into the Ag. When an occasional misaligned grain grows at a significant angle to the sheath, it evidently can penetrate the Ag sheath.²¹ Thus, the mechanical deformation process is unlikely to lead to grain

alignment in samples in which the 2212 phase is completely melted.

A second question concerns the atomic scale faceting which was apparent, both for the obliquely penetrating and for the almost parallel BSCCO grains. Indeed, Fig. 2 shows that the BSCCO produces microfacets so as to maximize the contact area between the Bi-O layer and the Ag. This suggests that the (001) BSCCO faced interfaces might have lower free energy than higher index plane facets do. However, the observed facet morphology also could be due to the anisotropic growth kinetics of Bi-2212. In this case, the steps would be due to cessation of growth of rapidly growing (001) planes.

A third question concerns the universal appearance of the half unit cell of Bi-2201 phase between the Ag and the Bi-2212. Ag lowers the melting point of a 2212 phase mixture¹⁷ and tends to produce a Bi-rich liquid from which the 2201 phase might form naturally. However, it is remarkable that the 2201 lattice spacing occurs only over one half of a unit cell and in direct proximity to the Ag (as demonstrated in Fig. 2). For example the arrowed Bi-2201 layer at point A in Fig. 2 transforms to Bi-2212 at point B, where this layer is no longer in direct contact with the Ag. In short, the Bi-2201 half-layer shows exactly the same stepped microstructure as the BSCCO/Ag interface. This observation provides support for the intrinsic stability of a single Bi-2201 at the Bi-2212/Ag interface. This very local change does make it appear that the Bi-2201 layer is produced by interface proximity. Nevertheless half cell, single half layer intergrowths of Bi-2201 phase were also common in the bulk of the grains.

In summary, we have shown by HRTEM that the Ag-BSCCO interface is always free of nonsuperconducting phases and generally well bonded. There is a very strong tendency for the (001) planes of the BSCCO to align parallel to the Ag interface and for microfaceting, which accommodates small misalignments of the (001) BSCCO planes. The interface phase always consists of a one half unit cell structure having the 2201-BSCCO lattice spacing.

We thank R. Ray II and E. E. Hellstrom (UW) for the 2212 tape and helpful discussions, and M. P. Frongillo

(Center for Materials Science and Engineering Electron Microscope Facility at MIT) for assistance with the HRTEM. This work has been sponsored by DARPA Contract N00014-90-J-4115 and EPRI Contract RP8009-05. The microscope facility at MIT is funded by the NSF-MRL Program and the microscopy work here was funded partially by DOE Contract DE-FG02-85ER45179.

- ¹M. Ueyama, T. Hikata, T. Kato, and K. Sato, *Jpn. J. Appl. Phys.* **30**, L1384 (1991).
- ²K. Heine, J. Tenbrink, and M. Thoner, *Appl. Phys. Lett.* **55**, 2441 (1989).
- ³Y. Yamada, B. Obst, and R. Flukiger, *Super. Sci. Technol.* **4**, 165 (1991).
- ⁴P. Haldar, J. G. Hoehn, Jr., J. A. Rice, M. S. Walker, and L. R. Motowidlo, *Appl. Phys. Lett.* **60**, 495 (1992).
- ⁵N. Enomoto, H. Kikuchi, N. Uno, H. Kumakura, K. Togano, and N. Watanabe, *Jpn. J. Appl. Phys.* **29**, L447 (1990).
- ⁶H. Kumakura, K. Togano, D. R. Dieterich, H. Maeda, J. Kase, and T. Morimoto, *IEEE Trans. Magn.* **27**, 1250 (1991).
- ⁷J. M. Tarascon, Y. Le Page, P. Barboux, B. G. Bagley, L. H. Green, R. McKinnon, G. W. Hull, M. Giroud, and D. M. Huang, *Phys. Rev. B* **37**, 9382 (1988).
- ⁸Y. Matsui and S. Horiuchi, *Jpn. J. Appl. Phys.* **27**, 2306 (1988).
- ⁹M. R. DeGuire, N. P. Bansal, D. E. Farrell, V. Finan, C. J. Kim, B. J. Hills, and C. J. Allen, *Physica C* **179**, 333 (1991).
- ¹⁰K. Schulze, P. Majewski, B. Hettich, and G. Petzow, *Z. Metallkd.* **81**, 836 (1990).
- ¹¹F. H. Chen, H. S. Koo, and T. Y. Tseng, *Appl. Phys. Lett.* **58**, 637 (1991).
- ¹²S. Nagai, N. Fujimura, T. Ito, and K. Shiraishi, *Jpn. J. Appl. Phys.* **30**, L826 (1991).
- ¹³R. Flukiger, T. Graf, M. Decroux, C. Groth, and Y. Yamada, *IEEE Trans. Magn.* **27**, 1258 (1991).
- ¹⁴J. Tenbrink, M. Wilhelm, K. Heine, and H. Kranth, *IEEE Trans. Magn.* **27**, 1239 (1991).
- ¹⁵T. E. Jones, J. W. Schindler, R. D. Boss, P. M. Thibado, and W. C. McGinnis, *Phys. Rev. B* **41**, 7191 (1990).
- ¹⁶J. Kase, K. Togano, H. Kumakura, D. R. Dieterich, N. Irisawa, T. Morimoto, and H. Maeda, *Jpn. J. Appl. Phys.* **29**, 1096 (1990).
- ¹⁷J. Kase, T. Morimoto, K. Togano, H. Kumakura, D. R. Dieterich, and H. Maeda, *IEEE Trans. Magn.* **27**, 1254.
- ¹⁸D. J. Brauer, R. Eujen, and J. Hudepohl, *IEEE Trans. Magn.* **27**, 1105 (1991).
- ¹⁹Y. Feng, K. E. Hautanen, Y. E. High, D. C. Larbalestier, R. Ray II, E. E. Hellstrom, and S. E. Babcock, *Physica C* **192**, 293 (1992).
- ²⁰R. Ray II and E. E. Hellstrom, *Physica C* **175**, 255 (1991).
- ²¹R. Ray II and E. E. Hellstrom, *Physica C* **172**, 435 (1991).